Peptide Design

Combination of Phage Display and Molecular Grafting Generates Highly Specific Tumor-Targeting Miniproteins**

Frederic Zoller, Annette Markert, Philippe Barthe, Wenye Zhao, Wilko Weichert, Vasileios Askoxylakis, Annette Altmann, Walter Mier, and Uwe Haberkorn*

Peptides are of growing interest as a non-immunoglobulin alternative for the development of new molecular entities.[1] Disulfide-stabilized miniproteins are a class of peptides that represent an ideal template for the development of stable affinity reagents in drug design,[2] molecular diagnostics, and targeted therapy.[3,4] This is due to their outstanding proteolytic stability, their small size, and especially their tolerance to mutagenesis.[3,4]

These structural characteristics also make disulfide-stabilized miniproteins suitable candidates for use in the scaffold method, that is, the integration of an affinity function into a well-defined, stably folded structural framework by locally reshaping its primary structure,[5] which in itself is a promising approach for the design of new binding motifs and to stabilize linear peptide binders.[6] Disulfide-stabilized miniproteins could therefore be used as scaffolds for combinatorial peptide library construction, such as phage display for the screening of huge molecular repertoires of potential binders against virtually any given target.[7,8] Herein, we used the disulfide-stabilized miniprotein Min-23 as a molecular scaffold in a phage display approach to generate a combinatorial library for the identification of new affinity functions against the angiogenesis marker delta-like ligand 4 (Dll4).

Min-23 is a two disulfide-bridge stabilized scaffold, which was rationally designed by miniaturization of its parent knottin *Ecballium elaterium* trypsin inhibitor II (EETI-II).[9] Min-23 offers outstanding proteolytic stability and beneficial pharmacokinetic properties for in vivo applications including molecular imaging.[10] Furthermore, Min-23 has already been applied successfully as a structural template for phage display by insertion of up to ten amino acids into its hypervariable, surface-exposed GPNG loop.[11] However, random amino acid substitutions within disulfide-constrained proteins often

negatively influence the synthesis yield, because autonomous folding results in regioisomer formation owing to incorrect disulfide connectivity, and requires the appropriate oxidative folding methods.[10,12,13] Therefore, we combined the Min-23 based phage-display technology with a different peptide scaffold—the sunflower trypsin inhibitor (SFTI-I)—to generate a readily accessible peptide format for hit-to-lead development in vitro and in vivo.

SFTI-I is a cyclic 14-residue peptide with a single disulfide bridge, isolated from sunflower seeds.[14] In various studies, the suitability of SFTI-I as a scaffold for the development of peptide-based drug candidates was investigated.[15] It has been shown, that the KSIPPI-domain, known as the binding loop, is tolerant to amino acid substitutions[16] and allows for the integration of binding epitopes.[6] Moreover, backbone modifications and labeling concepts have been developed to facilitate the in vivo application of SFTI-I derivatives, which have used the acyclic as well as the head-to-tail cyclic variants.[17]

The cell membrane protein Dll4 is highly overexpressed on endothelial and tumor cells and highly involved in angiogenic balance by binding to the Notch-1 receptor. Blockage of the Dll4/Notch-1 interaction initiates nonproductive tumor vascularization and causes a delay of tumor growth.[18,19] Thus, this pathway is a promising target for cancer therapy and molecular diagnosis of tumor angiogenesis.[20,21]

Screening of a combinatorial Min-23 phage-display library, which incorporates a random peptide sequence of eight residues between Cys[16] and Phe[25], a Dll4-specific binding domain was identified (sequence of the screening hit: H₂N-LMRCKQDSDCLAGSVC**LFHLFIYI**FCG-COOH, binding residues shown in bold, further details are

---

[*] Dr. F. Zoller,[+] Dr. A. Markert,[+] Dr. V. Askoxylakis, Dr. A. Altmann
DKFZ, Klinische Kooperationseinheit Nuklearmedizin
Im Neuenheimer Feld 280, 69120 Heidelberg (Germany)

Dr. P. Barthe
Centre de Biochimie Structurale, Institut National pour la Santé et la Recherche Médicale U1054, Centre National pour la Recherche Scientifique Unité Mixte de Recherche 5048,
Université Montpellier 1 and 2, 34090 Montpellier (France)

Prof. Dr. W. Weichert
Universitätsklinik Heidelberg, Institut für Pathologie
Im Neuenheimer Feld 220, 69120 Heidelberg (Germany)

W. Zhao, Dr. W. Mier, Prof. Dr. U. Haberkorn
Universitätsklinik Heidelberg
Radiologische Klinik, Abteilung Nuklearmedizin
Im Neuenheimer Feld 400, 69120 Heidelberg (Germany)
E-mail: uwe.haberkorn@med.uni-heidelberg.de

given in the Supporting Information). However, the chemical synthesis of this Min-23 derivative resulted in a poor yield because of precipitation and formation of regioisomers during the folding process. To overcome these limitations, the binding residues of the Min-23 phage-display-evolved peptide were transferred into the variable loop of the SFTI-I. On the contrary, phage-display screening using an SFTI-I scaffold library directly did not yield a Dll4-positive binding species (Supporting Information).

In contrast to making multiple disulfide-constrained peptides, this approach allowed highly reliable chemical synthesis of the SFTI-I derivate using automated solid-phase peptide synthesis (SPPS) followed by iodine oxidation of the fully deprotected peptide in solution (Scheme 1). The
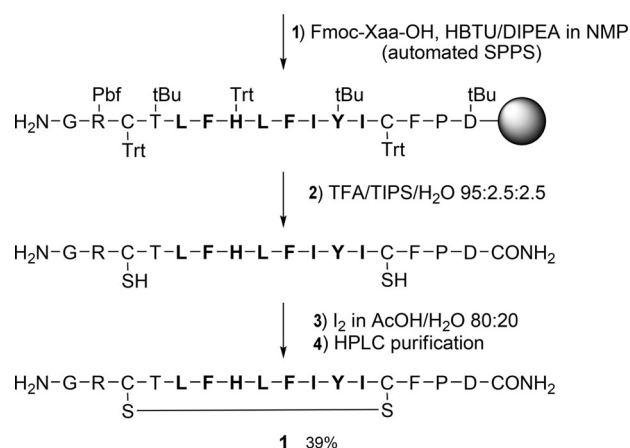
Scheme 1. Synthesis of SFTI-I miniproteins. The synthesis route as shown for compound **1** was applied for all SFT-I derivatives in this study. DIPEA = diisopropylethylamine, Fmoc = fluorenylmethoxy carbonyl, HBTU = O-(benzotriazol-1-yl)-N,N,N',N'-tetramethyluronium hexafluorophosphate, NMP = N-methylpyrolidone, Pbf = 2,2,4,6,7-pentamethyldihydrobenzofuran-5-sulfonyl, tBu = $tert$-butyl, TFA = trifluoro acetic acid, TIPS = triisopropyl silane, Trt = trityl.

single disulfide bridge was formed within one to two hours at ambient temperature in dilute acetic acid, resulting in overall yields up to 39% and high purity (>95%). The improved synthesis of SFTI-I peptides also enabled convenient chemical modifications including amino acid substitutions and fluorescent- or radiolabeling for in vitro and in vivo characterization (Supporting Information).

Hence, the molecular grafting strategy by integration of an identified binding site into the structurally defined scaffold SFTI-I represents a promising approach to rationally design a small, highly stable miniprotein. This concept offers a reliable hit-to-lead development of new peptide entities with easy synthesis and high yields as compared to the complex synthesis of Min-23. Currently, this scaffold strategy is being pursued for the engineering of SFTI-I binders against other tumor associated targets, such as B7-H3, that were identified by in vitro display screening techniques (data not shown).

Surface plasmon resonance (SPR) spectroscopy was performed to verify the specificity of **1** for Dll4. The acyclic

SFTI-I **10** and the receptor Notch-1 were used as controls. Specific binding interactions with the recombinant fusion protein Dll4-Fc were only observed for miniprotein **1**, with a K_D value of 22 nM (Figure 1; Fc = a region of human IgG1). The influence of the individual amino acids on the Dll4-binding properties was investigated by single-residue substi-
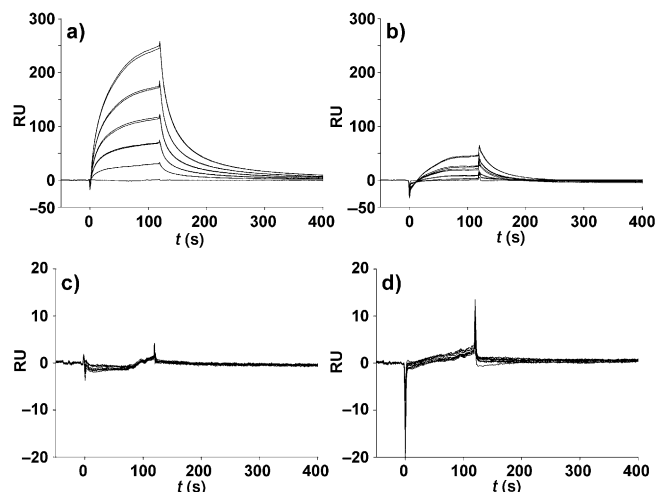

Figure 1. Surface plasmon resonance (SPR) analysis (RU = response units). The miniprotein **1** (a, b) and the unmodified scaffold **10** (c, d) were tested with the recombinant fusion protein Dll4-Fc (a, c) and Notch-1 (b, d) as control. The proteins were immobilized on a Biacore CM5 sensor chip and the peptide concentrations were: 0.25, 0.5, 0.75, 1, 1.25 μM (n = 2). Kinetic data from the SPR measurements are given in Table 1.

tution by alanine of the binding domain spanned by the residues Thr[4] to Cys[13]. SPR analysis was also conducted to demonstrate the pharmacological activity of peptide **1** as a potential inhibitor of the Dll4/Notch-1 interaction (Supporting Information).

The resulting eight disulfide-stabilized, alanine substituted peptides **2–9** were analyzed by SPR and their ^{125}I-labeled derivatives were used in cell-binding assays with the Dll4-positive cell line PC-3 (Supporting Information). In both experiments, substitution with alanine had a significant effect on the Dll4-binding capability of the miniprotein (Table 1). Substitution of the lipophilic functions (Phe[6,9]; peptides **3** and **6**, and Ile[10,12]; peptides **7** and **9**) resulted in a loss of binding potential compared to the unmodified peptide **1**. Replacement of Leu[5], His[7], and Leu[8] (peptides **2**, **4**, and **5**) by alanine resulted in decreased binding affinities (higher K_D values) and moderate cellular binding ratios as compared to **1**.

The cellular binding capability of the SFTI-I derivatives was determined by applying fluorescently labeled (5(6)FAM; Figure 2) and radiolabeled peptides to different Dll4-expressing cell lines (Supporting Information). Fluorescent staining of HUVECs and PC-3 cells clearly showed the cell-membrane binding of 5(6)FAM-**1b** compared to the alanine-mutated derivative 5(6)FAM-**6**. Competition for binding with the unlabeled peptide **1** resulted in a significant decrease in green fluorescence intensity. These results were confirmed by flow cytometry (Figure 2). 5(6)FAM-**1b** was observed to have the

Table 1: Summary of SPR analysis and cellular binding of the SFTI-I derivatives **1–11**.

Peptide	Binding motif[a]	K_{on}[b] [$M^{-1}s^{-1}$]	K_{off}[b] [s^{-1}]	K_D[b] [nM]	Cellular-binding ratio[c]
1	LFHLFIYI	5.56×10^5	0.0121	22	1.00 ± 0.02
1 b[d]	LFHLFIYI	1.60×10^4	0.0014	88	0.70 ± 0.05
2	**A**FHLFIYI	5.34×10^4	0.0273	511	0.51 ± 0.03
3	LA**H**LFIYI	n.b.	n.b.	n.b.	0.38 ± 0.02
4	LF**A**LFIYI	7.25×10^4	0.0121	167	1.08 ± 0.08
5	LFH**A**FIYI	3.22×10^4	0.0214	665	0.58 ± 0.04
6	LFHL**A**IYI	n.b.	n.b.	n.b.	0.27 ± 0.01
7	LFHLF**A**YI	n.b.	n.b.	n.b.	0.32 ± 0.02
8	LFHLFI**A**I	n.b.	n.b.	n.b.	–/–
9	LFHLFIY**A**	n.b.	n.b.	n.b.	0.42 ± 0.01
10[e]	KSIPPI	n.b.	n.b.	n.b.	0.01 ± 0.01
11	**N**FH**N**FIYI	5.90×10^4	0.0012	20	0.71 ± 0.04

[a] Binding motifs are framed by the residues H₂H-Gly-Arg-Cys-Thr- and -Cys-Phe-Pro-Asp-CONH₂ of the disulfide-stabilized SFTI-I scaffold. [b] Kinetic data from SPR measurments were determined with immobilized fusion protein Dll4-Fc (loading level = 8690 RU); n.b.: no binding detected. Applied peptide concentrations: 0.25, 0.5, 0.75, 1, 1.25 μM (n = 2). [c] Cellular-binding capability to PC-3 cells was determined by incubation with ^{125}I-labeled peptides. Cellular-binding ratio = (% binding/dose/10^6 cells of peptide X)/(% binding/dose/10^6 cells of **1**); X = peptide **1–11** (mean ± SD; n = 3). [d] Peptide **1 b** was labeled with 5(6)-carboxyfluorescein (5(6)FAM) at the N-terminus. [e] The acyclic derivative of SFTI-I was used, and the Phe^{12} residue was substituted by Tyr^{12} for radioiodination.

highest cell-bound fluorescence, whereas 5(6)FAM-**6** had the lowest signal at 52 ± 1%. Competition with unlabeled peptide **1** led to 39 ± 5% inhibition of cellular binding (Supporting

Information). These in vitro studies confirm the binding specificity of **1** for Dll4.

The proteolytic stability of miniprotein **1** was determined by incubation of the ^{125}I-labeled derivatives in human serum. Radio-HPLC analysis of the serum aliquots showed high stability of the full-length peptide ^{125}I-(Tyr^{11})-**1** over a period of ten days. In contrast, the non-stabilized, linear binding sequence ^{125}I-(Tyr^7)-LFHLFIYI showed a half-life in human serum of 2.2 hours. Prolonged incubation led to proteolytic fragmentation, as indicated in the HPLC elution profiles by the presence of metabolites with shorter retention times (Supporting Information). The biotinylated peptide **1** showed a strong membrane-associated immunohistochemical signal in vascular endothelium and tumor cells of AR42J tumor tissue. This histological corroboration highlights the potential of the generated peptide for application in molecular diagnostics (Figure 3 a,b).

The in vivo tumor-targeting potential of the peptides was determined by biodistribution profiling of the ^{131}I-labeled SFTI-I derivatives in AR42J tumor-bearing mice (Figure 3 c). The designed miniprotein **1** demonstrated a maximum tumor accumulation of 0.50 ± 0.08 % ID/g (percent injected dose per gram of tissue). High concentrations of radioactivity were found in the liver, as a result of the lipophilic character of **1**. To increase the peptide concentration in the blood pool and to enable prolonged availability for tumor accumulation, the lipophilicity of the peptide was reduced by polar isosteric substitution of the leucine residues Leu^5 and Leu^8 by asparagine (**11**). The Dll4-binding capability of peptide **11** was verified by SPR (Table 1) and cellular binding assays
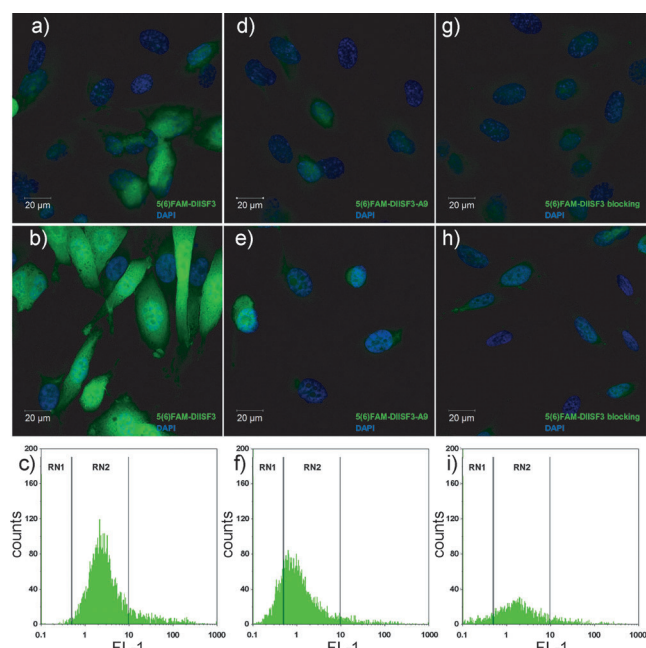

Figure 2. Cellular staining of fluorescently labeled miniproteins. Representative confocal microscopy images and flow cytometry counts of 5(6)FAM-**1 b** (a–c), 5(6)FAM-**6** (d–f), and 5(6)FAM-**1 b** after blocking with unlabeled **1** (g–i). HUVEC cells (a, d, g) and PC-3 cells (b, c, e, f, h, i) were used. 5(6)FAM-labeled peptides (green) were co-stained with DAPI (blue) for visualization of the nuclei. Scale bar = 20 μm. Dll4 expression in the selected cell lines was validated by RT-PCR and Western blot (Supporting Information).
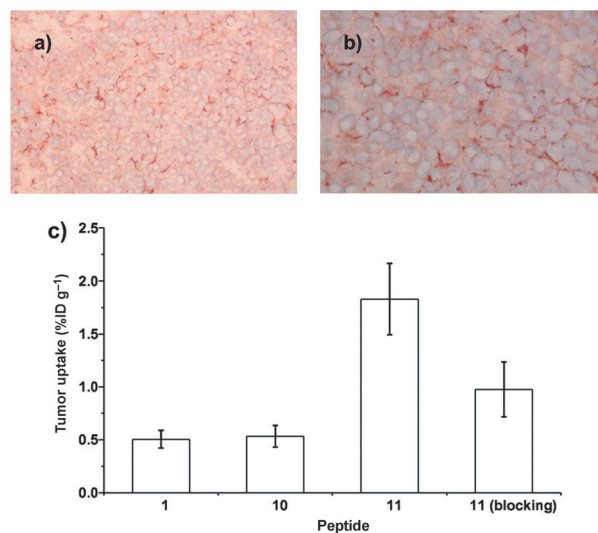

Figure 3. Immunohistochemical staining and in vivo tumor-targeting properties of radiolabeled peptides. a, b) Immunostaining with biotinylated peptide **1** on AR42J tumor tissue cryosections taken from mice (overview, ×20 (a) and high-power view, ×40 (b)). c) Tumor-targeting properties of the radiotracer 120 min after intravenous administration were determined by organ biodistribution in AR42J tumor-bearing mice. Tumor uptake of the miniprotein ^{131}I-(Tyr^{11})-**1**, the unmodified scaffold ^{131}I-(Tyr^{12})-**10**, the polar isosteric analogue ^{131}I-(Tyr^{11})-**11**, and its competition with unlabeled **11** are shown (mean ± SD; n = 3). Full biodistribution data are given in the Supporting Information.

(Supporting Information). The tumor uptake of ^{131}I-(Tyr^{11})-**11** increased to a maximum of $1.83 \pm 0.34\,\%\,ID/g$, and could be blocked by co-administration of unlabeled **11** (51 % inhibition of tumor uptake). In contrast, the unmodified scaffold ^{131}I-(Tyr^{12})-**10** demonstrated a tumor accumulation of only $0.53 \pm 0.10\,\%\,ID/g$ at the selected time point (Figure 3c).

In conclusion, this study validates the molecular-grafting concept for the development of new molecular entities for therapeutic use. It was shown that the binding specificity against the selected tumor-associated target was preserved by transferring the phage-display-identified binding domain from Min-23 into the SFTI-I peptide. Both the Dll4-binding specificity and the tumor-targeting capability of the rationally designed miniprotein were confirmed in vitro and in vivo. However, further optimization is required to improve the tumor accumulation of this novel anti-angiogenic drug candidate. This design approach might facilitate the hit-to-lead development of other previously identified affinity functions in drug design.

[1] H. K. Binz, P. Amstutz, A. Pluckthun, *Nat. Biotechnol.* **2005**, *23*, 1257.

[2] D. J. Craik, R. J. Clark, N. L. Daly, *Expert Opin. Invest. Drugs* **2007**, *16*, 595.

[3] F. Zoller, U. Haberkorn, W. Mier, *Molecules* **2011**, *16*, 2467.

[4] A. Skerra, *Curr. Opin. Biotechnol.* **2007**, *18*, 295.

[5] P. A. Nygren, A. Skerra, *J. Immunol. Methods* **2004**, *290*, 3.

[6] L. Y. Chan, S. Gunasekera, S. T. Henriques, N. F. Worth, S. J. Le, R. J. Clark, J. H. Campbell, D. J. Craik, N. L. Daly, *Blood* **2011**, *118*, 6709.

[7] G. P. Smith, V. A. Petrenko, *Chem. Rev.* **1997**, *97*, 391.

[8] A. Marr, A. Markert, A. Altmann, V. Askoxylakis, U. Haberkorn, *Methods* **2011**, *55*, 215.

[9] A. Heitz, D. Le-Nguyen, L. Chiche, *Biochemistry* **1999**, *38*, 10615.

[10] F. Zoller, T. Schwaebel, A. Markert, U. Haberkorn, W. Mier, *ChemMedChem* **2012**, *7*, 237.

[11] C. Souriau, L. Chiche, R. Irving, P. Hudson, *Biochemistry* **2005**, *44*, 7143.

[12] N. L. Daly, S. Love, P. F. Alewood, D. J. Craik, *Biochemistry* **1999**, *38*, 10606.

[13] O. Avrutina, H. U. Schmoldt, D. Gabrijelcic-Geiger, D. Le Nguyen, C. P. Sommerhoff, U. Diederichsen, H. Kolmar, *Biol. Chem.* **2005**, *386*, 1301.

[14] S. Luckett, R. S. Garcia, J. J. Barker, A. V. Konarev, P. R. Shewry, A. R. Clarke, R. L. Brady, *J. Mol. Biol.* **1999**, *290*, 525.

[15] M. L. Korsinczky, H. J. Schirra, D. J. Craik, *Curr. Protein Pept. Sci.* **2004**, *5*, 351.

[16] N. L. Daly, Y. K. Chen, F. M. Foley, P. S. Bansal, R. Bharathi, R. J. Clark, C. P. Sommerhoff, D. J. Craik, *J. Biol. Chem.* **2006**, *281*, 23668.

[17] R. G. Boy, W. Mier, E. M. Nothelfer, A. Altmann, M. Eisenhut, H. Kolmar, M. Tomaszowski, S. Kramer, U. Haberkorn, *Mol. Imaging Biol.* **2010**, *12*, 377.

[18] J. Ridgway, G. Zhang, Y. Wu, S. Stawicki, W. C. Liang, Y. Chantery, J. Kowalski, R. J. Watts, C. Callahan, I. Kasman, M. Singh, M. Chien, C. Tan, J. A. Hongo, F. de Sauvage, G. Plowman, M. Yan, *Nature* **2006**, *444*, 1083.

[19] I. Noguera-Troise, C. Daly, N. J. Papadopoulos, S. Coetzee, P. Boland, N. W. Gale, H. Chieh Lin, G. D. Yancopoulos, G. Thurston, *Nature* **2006**, *444*, 1032.

[20] N. S. Patel, J. L. Li, D. Generali, R. Poulsom, D. W. Cranston, A. L. Harris, *Cancer Res.* **2005**, *65*, 8690.

[21] D. J. Hicklin, *Nat. Biotechnol.* **2007**, *25*, 300.